Aeroacoustics Conferences
30 May - 1 June, 2016, Lyon, France
22nd AIAA/CEAS Aeroacoustics Conference

Broadband liner impedance eduction for multimodal acoustic propagation in the presence of a mean flow

Renata Troian[*], Didier Dragna[†], Christophe Bailly[‡], Marie-Annick Galland[§]
Laboratoire de Mécanique des Fluides et d'Acoustique
UMR CNRS 5506, École Centrale de Lyon, 69134 Ecully, France
Marc Versaevel[¶]
SAFRAN - Aircelle, 76700 Gonfreville l'Orcher, France
and Rik Wijntjes[‖]
NLR, 8316PR, Marknesse, The Netherlands

This study deals with a broadband impedance eduction method developed to identify the surface impedance of acoustic liners, mounted in the walls of aircraft engine nacelles, from measurements on a test rig. A numerical model of an acoustic liner under a grazing flow is undertaken by considering finite-difference time-domain simulations and the Euler equations for the acoustic propagation. A broadband impedance model is used to prescribe time-domain boundary conditions. The impedance eduction procedure is based on insertion loss and pressure measurements and is obtained by using a multiobjective optimization involving the genetic algorithm NSGA-II. Insertion loss measurements for two liners performed in Netherlands Aerospace Center are presented, as well as liners' impedance predicted using a semi-empirical model. A good agreement between measurements and acoustic propagation simulations is observed for $M = 0$ and $M = 0.3$.

I. Introduction

Numerous inverse techniques for impedance eduction were developed recently to satisfy the industrial needs of the liner impedance identification before using it in the aircraft. These methods are performed through the measurement of the acoustic field at selected locations outside the liner and have the advantage of not destroying the liner sample. The acoustic propagation in the lined duct for a given geometry of the liner must be simulated first. Approaches based on linearized Euler equations resolution use the finite element[1,2,3,4] or the finite-difference method[5,6] for numerical simulations. Helmholtz equations are considered in the mode matching models.[7,8] Test rigs were constructed as well to provide the input data for the impedance eduction. A simple test rig for measuring the impedance of the liner is a normal incidence tube. In such facility the liner impedance can be identified for acoustic propagation without flow. The two-microphone method is often employed in this case. An example of such measurements can be found in Schultz et al.[9] Two normal-incidence impedance tubes (NIT) are presented. The NIT of the University of Florida and NASA NIT. For both rigs plane acoustic propagation is considered. Detailed characteristics can be found in table 1.

Properties of liners mounted in the nacelle can differ much from those measured in a NIT. Among the possible explanation the presence of a grazing flow and installation effects are often highlighted. Standard rigs

[*]Postdoctoral fellow, corresponding author: renata.troian@ec-lyon.fr
[†]Assistant professor.
[‡]Professor, Senior AIAA Member.
[§]Professor.
[¶]Acoutic specialist.
[‖]R&D Engineer.

have been improved, and a new generation of facilities with grazing flow was developed and used for liner impedance eduction. Over the last three decades, the NASA Langley Liner Physics Team has constructed series of test rigs suitable for evaluation of acoustic liners in realistic aeroacoustic environments. With a grazing flow impedance tube (GFIT) of Langley NASA center a benchmark data was acquired and kindly provided for the research community for impedance eduction methods validation by Jones et al.[2] This apparatus has a 50.8 mm to 50.8 mm cross-section with a source upstream of the liner and a near-anechoic termination downstream of the liner. Mean flows up to Mach 0.4 can be achieved in the test section containing the acoustic liner. The channel is equiped with 96 microphones, including the reference microphone, and 31 microphones located on the wall opposite the liner are used in the impedance eduction process.
The German Aerospace Center (DLR) also built the DUct aCoustic Test rig with Square cross section (DUCT-S) to evaluate different liners, see Busse-Gerstrengarbe et al.[10] Several improvements of the DUCT-S lead to a redesigned version named DUct aCoustic Test rig with Rectangular cross section (DUCT-R). For the cross-sectional area of 60 mm to 80 mm a centerline Mach number of around 0.3 is achieved in the liner region. The upstream and downstream parts of the duct are divided into two microphone modules and a loudspeaker module. These modules contain an overall number of 106 microphone positions which are spread over the rig.

The presented above measurement rigs were designed for impedance identification methods that use the

Table 1. Characteristics of existing measurement rigs.

Duct	Cross-section, mm×mm	Frequency range, kHz	Mach number, max	Acoustic propagation
NIT, Florida[9]	25.4×25.4	[0.5; 6.7]	–	plane wave
NIT, NASA[9]	50.8×50.8	[0.5; 3]	–	plane wave
GFIT, NASA[2]	50.8×50.8	[0.5; 3]	0.4	plane wave
DUCT-R, DLR[10]	60×80	[0.2; 2.1]	0.3	plane wave
B2A, ONERA[11]	50×50	[1.; 3.1]	0.3	plane wave
UT of Compiegne[12]	200×100	[0.5; 2.5]	0.13	multimodal
NLR[13]	150×300	[0.5; 6]	0.7	multimodal

acoustic pressure for eduction process. Primus et al.[11] (ONERA) has developed an approach, based on non-intrusive Laser Doppler Anemometry (LDA) measurements of the acoustic velocity field above the liner surface in an aero-thermo-acoustic bench (B2A). The aeroacoustic test bench has a section 50 mm by 50 mm. The termination is equipped with a quasi-anechoic outlet, leading to upstream reflection coefficient smaller than 0.2 for frequencies higher than 500 Hz. A mean flow of bulk Mach number up to 0.3 can be provided.
The described above rigs with grazing flow present the conditions closer to realistic ones than the normal incident tube. But still not all the phenomena meet in the airplane nacelle are reproduced. Specifically, only plane wave propagation is considered. Recently, studies of an impedance eduction method for multimodal propagation were initiated. In the paper of Buot de l'Epine et al.[12] a rectangular duct with section dimensions 0.2×0.1 m is used for the eduction providing multimodal propagation conditions. The terminations of the experimental facility are not perfectly anechoic, and the reflection conditions at both ends have been measured to be taken into account in the propagation model. The liner is placed on the upper face of the test section. An eduction method, based on a Bayesian approach, is proposed to identify the liner impedance from sound pressure measured in the duct under multimodal propagation and grazing flow.
In this work, an eduction method suitable for multimodal acoustic propagation is proposed. The difference between measured and simulated insertion loss, together with the wall pressure in the duct, is minimized to identify the liner impedance. Concerning the numerical model, the linearized Euler equations are solved using a finite-difference time-domain algorithm. The experimental part is conducted in the measurements facility designed in Netherlands Aerospace Centre (NLR). The duct geometry leads to multimodal propagation starting from 570 Hz. The paper is organized as follows. First, the test rig is presented with the description of the investigated liners and conducted measurements. Then the numerical modeling of the acoustic propagation under the grazing flow in a rectangular lined duct together with impedance boundary condition is discussed. The impedance eduction method is presented in Section 3 with its validation for the

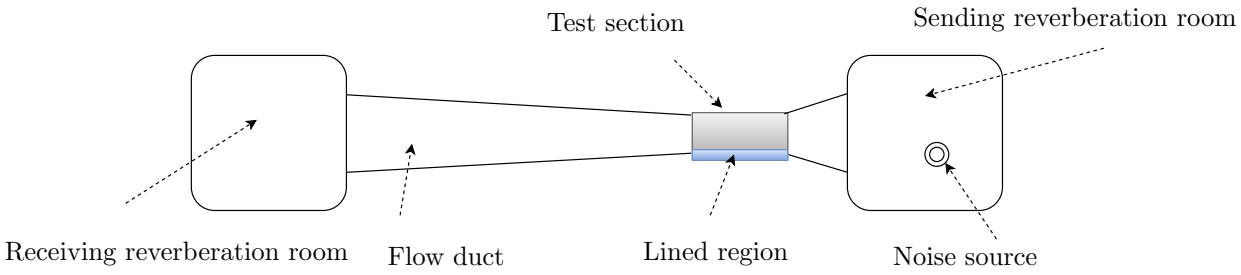

Figure 1. Sketch of the grazing flow impedance tube, NLR.

case of plane wave propagation. Results are presented in Section 4 and concluding remarks are provided in Section 5.

II. Experimental setup.

II.A. NLR test rig

Insertion loss measurements were performed in the Netherlands Aerospace Center flow duct facility (FDF)[13] (see figure 1). The measurements rig consists in two reverberation rooms, a flow duct and a test section. The cross-section of the test section is 0.15 m to 0.3 m and its length is 1.05 m. For each liner the measurements were performed using a broadband source. It was generated by 4 Monacor (type MRD-650) dynamics, 4 low frequency speakers and 8 Beyma tweeters (type CP22) placed in the sending reverberation room providing an in-duct sound field. Two rotating microphones measure the acoustic pressure inside the two reverberation rooms. The level of excitation was monitored in the sending room. It provides an overall SPL=130dB with broadband noise between 300 Hz and 10 kHz. In addition, acoustic pressure was measured inside the duct using six microphones situated in the test section opposite to the liner. Mach numbers up to 0.7 can be achieved either in the upstream or downstream flow directions. Background noise and flow noise corrections are accounted for.

II.B. Tested liners

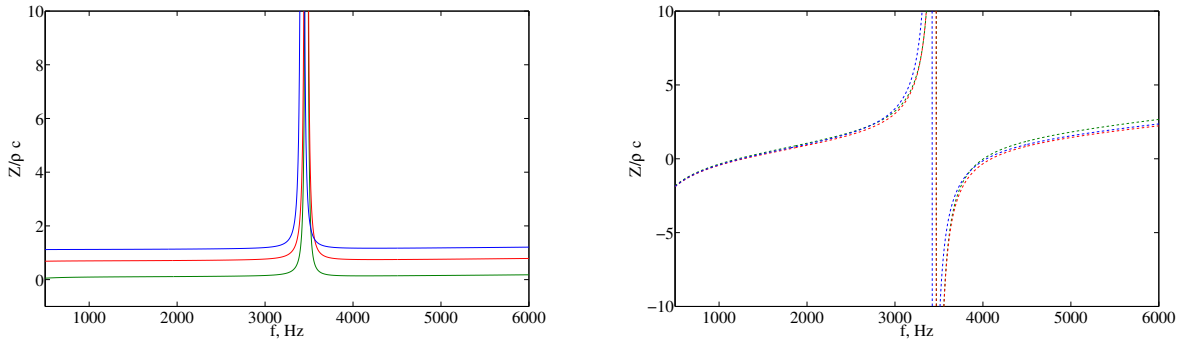

Figure 2. SDOF liner, real (a) and imaginary (b) parts of a predicted normalized admittance for $M = 0$ (green), 0.3 (red), 0.5 (blue).

Two reference liners were used for the study, a Single Degree of Freedom (SDOF) liner and a Double Degree of Freedom (DDOF) liner. The SDOF liner consists of a perforated plate glued to an honeycomb structure with a depth of 50 mm. The DDOF consists of two layers of honeycomb cells divided by a porous septum with total depth of 50 mm. Detailed parameters of liners cannot be given due to confidentiality

reasons.
The normalized admittance of the SDOF and DDOF liners predicted using a semi-empirical model for Mach numbers $M = 0;\ 0.3;\ 0.5$ is given in figures 2 and 3. It can be noticed that the real part of the impedance

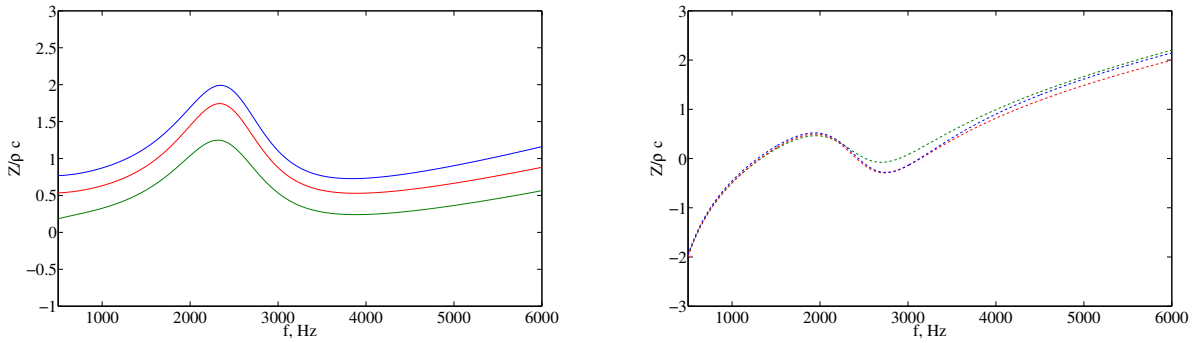

Figure 3. DDOF liner, real (a) and imaginary (b) parts of a predicted normalized admittance for $M = 0$ (green), 0.3 (red), 0.5 (blue).

is increasing with Mach number for both liners, leading to efficient attenuation in the flow cases. Resonance frequencies of the SDOF liner are observed at 1300 Hz and 4100 Hz, while the anti-resonance frequency is 3400 Hz, correspondingly to the liner depth. The first resonance frequency of the DDOF liner is 1300 Hz and coincides with the one of SDOF liner. The anti-resonance phenomena is not observed over the frequency range of interest leading to broadband attenuation of the DDOF liner.

II.C. Tests procedure and data processing

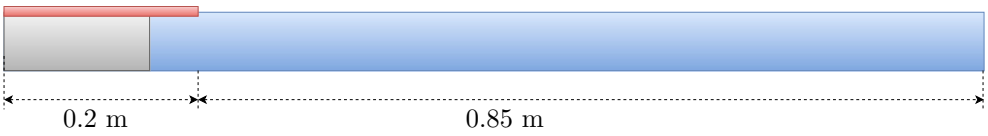

Figure 4. Sketch of the measurement configuration, SDOF and DDOF liners. Hard wall part is colored with dark gray, liner reference panel with blue and metallic tape with red.

SDOF and DDOF liner panels provided for measurements have 0.15 m width and 0.9 m length. Hard wall configuration and two lined configurations are tested (see schema presented in figures 4 and 5). A metallic tape is placed on the inlet part of the duct and 0.05 m of the liner thus providing the 0.2×0.15 m of inlet hard wall domain and 0.85×0.15 m of lined duct side. Measurements were conducted for $M = 0$, $M = 0.3$, $M = 0.5$.

For each data point auto- and cross-power spectra were acquired with a frequency step $\Delta f = 20$ Hz: moduli in dB, phase values in degrees and coherences. The background noise was measured and it was ensured that signal to noise ratio is on acceptable level. The transmission loss (TL) is determined by the difference between the averaged SPL measured in the sending and receiving reverberation rooms. The insertion loss (IL) is defined by the difference between the transmission loss measured with a hard-wall test section and the transmission loss measured with a lined section.

Insertion loss values for SDOF and DDOF liners are presented in figure 6. As can be seen, Il measurements are in accordance with predicted impedance values. The maximum attenuation is reached for the highest

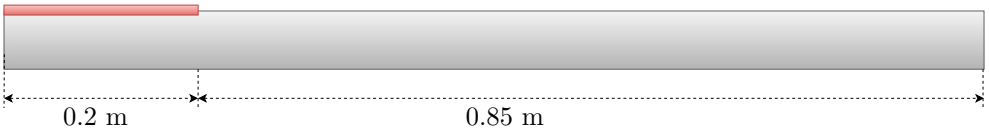

Figure 5. Sketch of the measurement configuration, hard wall. Hard wall part is colored with dark gray and metallic tape with red.

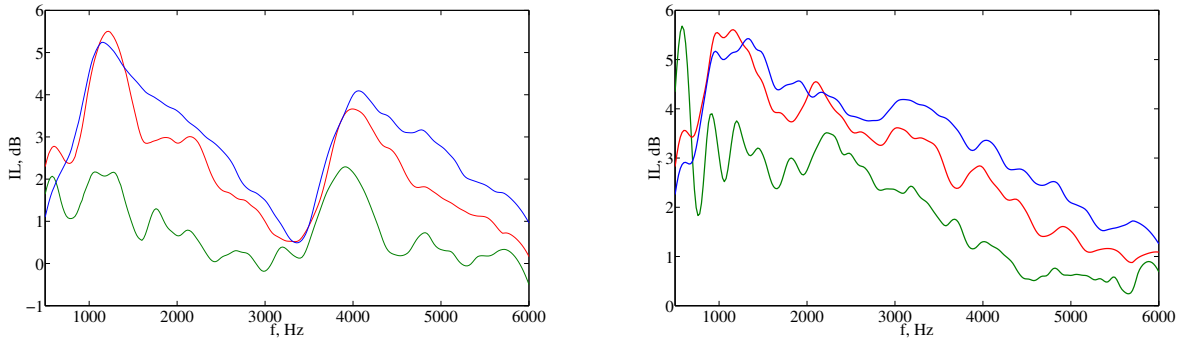

a) b)

Figure 6. Insertion loss measurements (dash lines) and smoothed data (solid lines) for M=0 (green), 0.3 (red), 0.5 (blue). SDOF liner(a) and DDOF liner (b).

Mach number ($M = 0.5$) for both liners while very low attenuation is observed for the no-flow configurations. IL for the SDOF liner has two peaks of absorption that corresponds to the resonance frequencies of the liner and equals to zero for the anti-resonance frequency. The DDOF liner is efficient on a broader frequency band.

III. Impedance eduction method

III.A. Computational model

The test section of the NLR rig is modeled by a rectangular duct for numerical simulations for the impedance eduction. Model includes a treated section and the presence of a mean flow. A sketch is given in figure 7.

The source and the exit planes of the computational domain are located at $x = 0$ and $x = L_x$, respectively. The dimensions of the duct cross-section are $L_y \times L_z$. The lower and two-side walls are rigid. The upper wall is also rigid except of the lined region ($L_1 < x < L_2$ in figure 7).
The frequency range is $500 \leq f \leq 6000$ Hz and the dimensions of the channel are $L_y = 0.15$ m and $L_z = 0.3$ m. The duct cut-on frequency for $M = 0$ is 570 Hz for no-flow case, which implies a multimodal propagation for $f > 570$ Hz.

III.B. Acoustic propagation in the lined duct

The three-dimensional Euler equations linearized around a given mean flow of density ρ_0 and velocity $\mathbf{V_0}$ are solved to determine the sound pressure field in the NLR lined duct. The mean pressure is assumed to be constant, the longitudinal pressure gradient is supposed to be small and the mean flow is homentropic. The acoustic velocity $\mathbf{v}$ and the acoustic pressure p are obtained by solving these equations written for an

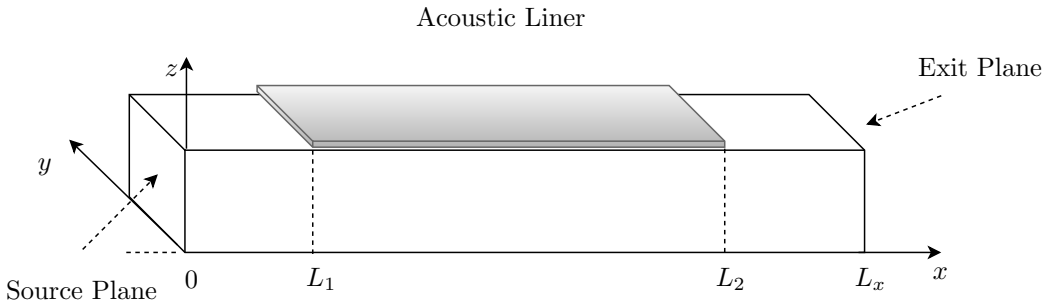

Figure 7. Sketch of the grazing flow impedance tube.

ideal gas

$$\frac{\partial p}{\partial t} + (\mathbf{V_0} \cdot \nabla)\, p + \rho_0 {c_0}^2 \nabla \cdot \mathbf{v} = \rho_0 {c_0}^2 Q \tag{1}$$

$$\frac{\partial \mathbf{v}}{\partial t} + (\mathbf{V_0} \cdot \nabla)\, \mathbf{v} + (\mathbf{v} \cdot \nabla)\, \mathbf{V_0} + \frac{1}{\rho_0} \nabla p = 0 \tag{2}$$

where c_0 is the speed of sound in air and Q is a source term, presented in a subsection III.E, generating an impulsive acoustic signal. These equations are discretized by low-dispersion and low-dissipation explicit numerical schemes, developed in computational aeroacoustics.[14,15] Optimized finite-difference schemes and selective filters over 11 points are used for spatial derivation and grid-to-grid oscillations removal, respectively. For the interior points, separated by at least five points from the boundary, the centered fourth-order finite-difference scheme of Bogey and Bailly[14] and the centered sixth order selective filter of Bogey et al.[16] are applied. For the boundary points in each direction, the eleven-point non-centered finite-difference schemes and selective filters of Berland et al.[15] are implemented. The optimized six-stage Runge-Kutta algorithm proposed by Bogey and Bailly[14] is used for time integration. The time-domain impedance boundary condition is presented in the next subsection. The inlet and outlet sections are assumed to be anechoic. Damping zones, including the non-reflecting boundary conditions of Bogey and Bailly[17] are thus implemented.

III.C. Broadband time-domain impedance boundary condition

The broadband impedance eduction method is developed in the time domain, thus avoiding the identification of the surface impedance for each frequency of interest. The surface impedance $Z(\omega)$ for a given angular frequency $\omega = 2\pi f$ is primarily defined in the frequency domain by $P(\omega) = Z(\omega)V_n(\omega)$, where $P(\omega)$ and $V_n(\omega)$ are the Fourier transforms of the acoustic pressure and normal acoustic velocity on the liner, respectively. The frequency-domain impedance boundary condition is translated into the time domain via the convolution product

$$p(t) = \int_{-\infty}^{t} v_n(t') z(t - t') \mathrm{d}t' \tag{3}$$

In order to be physically admissible in the time domain the analytical model is submitted to realizability conditions. Following Rienstra,[18] the impedance model must be causal and $z(t)$ must be real, which means $z(t) = 0$ for $t < 0$ and $Z(\omega)$ has to satisfy the reality condition $Z^*(\omega) = Z(-\omega)$. The condition $\mathrm{Re}[Z(\omega)] > 0$ has to be fulfilled as well for all $\omega \in \mathbb{R}$ since the impedance wall is passive. These conditions are not always satisfied by usual models defined in the Fourier space.[19] In the present study, a rational function of the form

$$Z\left(\omega\right) = \frac{a_0 + ... + a_N(-i\omega)^N}{1 + ... + b_N(-i\omega)^N} \tag{4}$$

is chosen. This formulation brings several advantages. A broadband impedance model is straightforwardly obtained, the convolution product can be performed at a small computational cost and finally, the coefficients

can be easily chosen to guarantee the impedance to be physically admissible. By using a partial fraction decomposition, the rational function can be written as a sum of first- and second-order systems

$$Z(\omega) = Z_\infty + \sum_{k=1}^{P} \frac{A_k}{\lambda_k - i\omega} + \sum_{k=1}^{S} \left(\frac{B_k + iC_k}{\alpha_k + i\beta_k - i\omega} + \frac{B_k - iC_k}{\alpha_k - i\beta_k - i\omega} \right) \tag{5}$$

Choosing $[Z_\infty,\ A_k,\ B_k,\ C_k] \in \mathbb{R}$ and $[\lambda_k,\ \alpha_k,\ \beta_k] \in \mathbb{R}^+$ ensure that the impedance model is causal and real. In addition, the passivity condition has to be checked for each set of the coefficients. This type of impedance model is also referred to as the multipole impedance model in the literature.[20]
The multipole impedance model (5) used in the present study is suitable for describing the classical liners with a few poles.

III.D. Impedance eduction procedure

The acoustic impedance is determined by minimizing an error function between the calculated and the measured sound field inside the channel. Most of the existing eduction methods are applied in the frequency range corresponding to plane wave propagation. Such configuration, however, is far from realistic conditions for liner applications. In this study a methodology, developed by Troian et al. in,[21] is presented for multimodal acoustic propagation. Multimodal propagation demands a larger number of microphones to capture variations in the pressure and velocity field, which leads to a significant additional cost. To overcome this difficulty, supplementary features of the sound field are examined for the eduction process. In particular, the duct insertion loss is considered in the present study. Therefore the objective function is formulated as follows

$$f_1(Z(\mathbf{X})) = \sum_{i=1}^{N_{IL}} \left(\mathrm{IL}_{\mathrm{measured}} - \mathrm{IL}_{\mathrm{FDTD}} \right)^2 \tag{6}$$

where $\mathbf{X} = [Z_\infty,\ A_k,\ B_k,\ C_k,\ \lambda_k,\ \alpha_k,\ \beta_k]$ are the coefficients of the multipole impedance model, $\mathrm{IL}_{\mathrm{measured}}$ and $\mathrm{IL}_{\mathrm{FDTD}}$ are the vectors of the insertion loss for the studied frequencies, obtained from the measurements and the simulations of the linearized Euler equations, N_{IL} is the number of selected frequencies.
The frequency subrange where only plane wave propagation occurs can again be considered to introduce an additional variable in the impedance eduction and to improve the robustness of the method. As an illustration, for the larger duct used for the validation of multimodal sound propagation, only plane waves propagate for $f \leq 550$ Hz. The objective function is

$$f_2(Z(\mathbf{X})) = \sum_{i=1}^{N_P} \sum_{l=1}^{M} \left\| p^i_{l\,\mathrm{measured}} - p^i_{l\,\mathrm{FDTD}} \right\|^2 \tag{7}$$

where $p^i_{l\,\mathrm{measured}}$ and $p^i_{l\,\mathrm{FDTD}}$ are the complex pressure values obtained from the measurements and from the numerical simulations, for microphone positions $l \in [1;\ M]$ and for a given frequency i. N_P is the number of considered frequencies, below the duct cut-off frequency, and therefore depends on the measurement facility.
Finally, the optimization problem to solve is expressed as

$$\begin{aligned}
&\min \quad && f_1(Z(\mathbf{X})) = \sum_{i=1}^{N_{IL}} \left(\mathrm{IL}_{\mathrm{measured}} - \mathrm{IL}_{\mathrm{FDTD}} \right)^2 \\
&\min \quad && f_2(Z(\mathbf{X})) = \sum_{i=1}^{N_P} \sum_{l=1}^{M} \left\| p^i_{l\,\mathrm{measured}} - p^i_{l\,\mathrm{FDTD}} \right\|^2 \\
&\text{such that} \quad && \underline{x}_j \leq x_j \leq \overline{x_j},\ \ \mathbf{X} = \{x_j\} \in \mathbb{R}^m \\
& && \mathrm{Re}(Z(\mathbf{X})) > 0
\end{aligned} \tag{8}$$

with $j = 1, .., m$, and where m is number of the impedance model coefficients to be identified. The variables $\mathbf{X}$ are usually restricted by side constraints $\underline{x}$ and $\overline{x}$, which are lower and upper limits that reflect the multipole model definition domain. The eduction method is conducted for the broadband impedance model, that is for all the frequencies simultaneously.
The set of the coefficients of the broadband impedance model that minimize the objective functions f_1 and f_2 must be identified. To deal with this multiobjective optimization problem the evolutionary genetic algorithm Non-dominated Sorting Genetic Algorithm-II (NSGA-II)[22] is employed that produces a set of Pareto optimal solutions.

III.E. Simulation parameters

The three-dimensional linearized Euler equations (1) and (2) are solved for the lined flow duct displayed in figure 7. A mean velocity of a following profile is imposed

$$V_{0\,x}(y,z) = Mc_0 \frac{2N_y+1}{2N_y}\left(1-\left|\frac{2y}{L_y}\right|^{2N_y}\right)\frac{2N_z+1}{2N_z}\left(1-\left|\frac{2z}{L_z}\right|^{2N_z}\right) \tag{9}$$

where $N_y = N_z = 6$. The computational area is discretized by $500 \times 57 \times 31$ points with a spatial step $\Delta x = 4.17 \times 10^{-3}$ m, $\Delta y = \Delta z = 5.2 \times 10^{-3}$ providing that acoustic waves are discretized by at least 10 point per wavelength. In the eduction process, the insertion loss is required. To calculate it, the acoustic field in the whole rigid and lined ducts has to be evaluated. In a rigid duct the acoustic field is decaying less rapidly with time that in a lined duct due to absence of an absorption treatment. Therefore, to capture the acoustic field as precisely as possible a longest simulation time is needed for the rigid duct configuration. The simulation is run up to $t_{max} = 0.04$ s for the case of rigid duct and $t_{max} = 0.02$ s for the case of lined duct with the step of $\Delta t = 1 \times 10^{-5}$ s. As an illustration, the computational time is about 10 min on a desktop computer for a single simulation (lined duct case). The impulse source term is defined by

$$Q(\mathbf{x},t) = \lambda(t)\exp\left(-\ln(2)\frac{(x-x_S)^2+(y-y_S)^2+(z-z_S)^2}{B^2}\right) \tag{10}$$

where the factor $\lambda(t)$ is given by

$$\lambda(t) = \frac{t-200\Delta t}{35\Delta t}\exp\left(-\ln(2)\frac{(t-200\Delta t)^2}{(35\Delta t)^2}\right) \tag{11}$$

The Gaussian half-width of the source is chosen to be $B = 5\Delta x$ and it is located at $(x_S;\ y_S;\ z_S) = (-0.05;\ 0;\ 0)$. Pressure and velocity in the frequency domain is obtained by Fourier transform of the time-domain solution.

IV. Data comparison

This section presents preliminary results obtained with direct calculations of acoustic propagation using the code presented in the section III. The SDOF and DDOF liners (figures 2 – 3) with an admittance model $Y(\omega)$ with $P = 0$ and $S = 2$ are considered. Hence,

$$Y(\omega) = \widetilde{Y}_\infty + \sum_{k=1}^{2}\left(\frac{\widetilde{B}_k + i\widetilde{C}_k}{\widetilde{\alpha}_k + i\widetilde{\beta}_k - i\omega} + \frac{\widetilde{B}_k - i\widetilde{C}_k}{\widetilde{\alpha}_k - i\widetilde{\beta}_k - i\omega}\right) \tag{12}$$

and the impedance is $Z(\omega) = 1/Y(\omega)$. The coefficients of the admittance expression are presented in Table 2. Insertion loss was calculated and compared with experimental data. Figure 8 presents the insertion

Liner	Mach	$\widetilde{Y}_\infty$	$\widetilde{B}_1$	$\widetilde{B}_2$	$\widetilde{C}_1$	$\widetilde{C}_2$	$\widetilde{\alpha}_1$	$\widetilde{\alpha}_2$	$\widetilde{\beta}_1$	$\widetilde{\beta}_2$
SDOF	M=0	0.00725	4095	1540	242.6	161.1	406.2	216.6	-7632	-25168
	M=0.3	0.01120	4803	1560	1744	1136	3191	1396	-7482	-25290
DDOF	M=0	0.09511	3281	3339	1671	-951.2	1710	2008	-7549	-19710
	M=0.3	0.11259	3039	3474	1651	207.8	2591	2807	-7041	-20588

Table 2. The coefficients of the broadband admittance model, SDOF and DDOF liner.

loss comparison for SDOF liner for $M = 0$ and $M = 0.3$. Insertion loss data for DDOF liner is presented in figure 9 for $M = 0$ and $M = 0.3$. Results of simulation correspond to the measured data for case with and without flow. Difference for high frequencies can be due to the impedance model. For SDOF liner attenuation for the no-flow case is not very significant and for $M = 0.3$ resonance and anit-resonance frequencies are observed. Behavior of the simulated IL for DDOF liner coincide with measurements. Results of eduction process for M=0; 0.3; 0.5 will be presented during the AIAA congress.

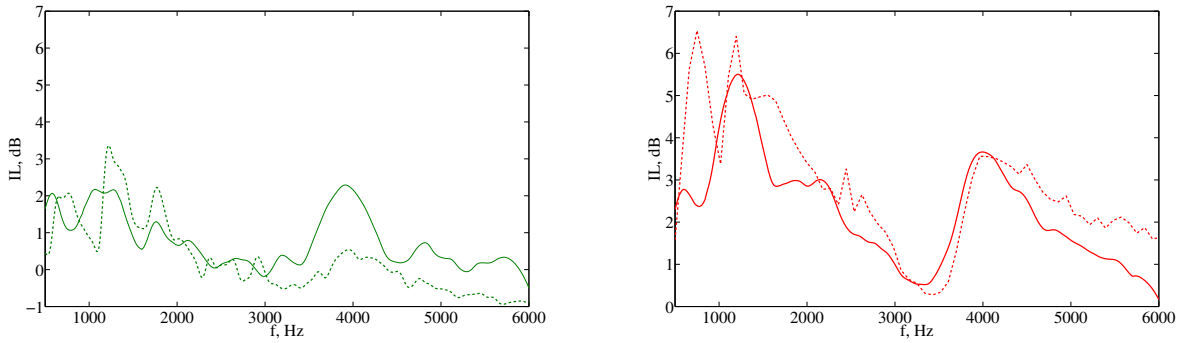

a) b)

Figure 8. Insertion loss, Measured data (solid line) vs numerical simultaion (dashed line), SDOF liner, M=0 (a), M=0.3 (b).

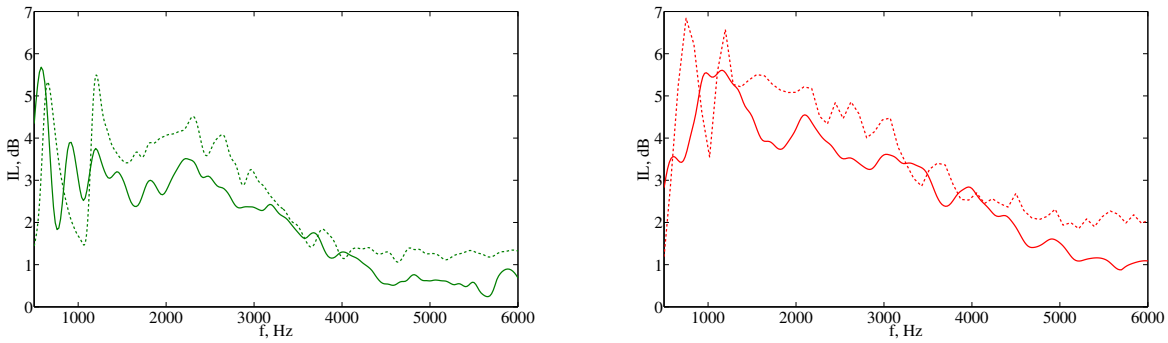

a) b)

Figure 9. Insertion loss, Measured data (solid line) vs numerical simultaion (dashed line), DDOF liner, M=0 (a), M=0.3 (b).

V. Concluding remarks

An impedance eduction method for the identification of the impedance characteristics of the acoustic liner in the duct under the grazing flow has been presented. The eduction process is based on minimization the measured and simulated values of insertion loss and pressure in the duct. The broadband impedance model is formulated in the time domain. The genetic optimization algorithm NSGA-II has been proposed for eduction itself. Measurements were conducted in NLR duct under the grazing flow conditions and multimodal acoustic propagation. SDOF and DDOF liners were tested for $M = 0;\ 0.3;\ 0.5$ and $f \in [500;\ 6000]$ Hz. Insertion loss measurements are in good agreement with simulation results. The results of eduction process will be presented in the AIAA 2016.

Acknowledgment

This work was performed within the framework of the Labex CeLyA of Université de Lyon, the program Investissements dAvenir (ANR-10-LABX-0060/ ANR-11-IDEX-0007) operated by the French National Research Agency (ANR). Research was carried on behalf of the European Project ENOVAL, and the authors would like to acknowledge Aircelle and NLR for the support. In addition, the authors would like to thank Dr. Michael Jones (NASA) for providing the benchmark data used the validation.

References

[1]Watson, W. R., Jones, M. G., Tanner, S. E., and Parrott, T. L., "Validation of a numerical method for extracting liner impedance," *AIAA Journal*, Vol. 34, No. 3, 1996, pp. 548–554.

[2]Jones, M. G., Watson, W. R., and Parrott, T. L., "Benchmark data for evaluation of aeroacoustic propagation codes

with grazing flow," *AIAA Paper*, Vol. 2853, 2005, pp. 2005.

[3]Eversman, W. and Gallman, J. M., "Impedance eduction with an extended search procedure," *AIAA Journal*, Vol. 49, No. 9, 2011, pp. 1960–1970.

[4]Primus, J., Piot, E., and Simon, F., "An adjoint-based method for liner impedance eduction: Validation and numerical investigation," *Journal of Sound and Vibration*, Vol. 332, No. 1, 2013, pp. 58–75.

[5]Reymen, Y., Baelmans, M., and Desmet, W., "Efficient implementation of Tam and Auriault's time-domain impedance boundary condition," *AIAA Journal*, Vol. 46, No. 9, 2008, pp. 2368–2376.

[6]Richter, C., Hay, J. A., Schönwald, N., Busse, S., Thiele, F., et al., "A review of time-domain impedance modelling and applications," *Journal of Sound and Vibration*, Vol. 330, No. 16, 2011, pp. 3859–3873.

[7]Elnady, T., Bodén, H., and Elhadidi, B., "Validation of an inverse semi-analytical technique to educe liner impedance," *AIAA Journal*, Vol. 47, No. 12, 2009, pp. 2836–2844.

[8]Sellen, N., Cuesta, M., and Galland, M.-A., "Noise reduction in a flow duct: Implementation of a hybrid passive/active solution," *Journal of Sound and Vibration*, Vol. 297, No. 3, 2006, pp. 492–511.

[9]Schultz, T., Liu, F., Cattafesta, L., Sheplak, M., and Jones, M., "A Comparison Study of Normal-Incidence Acoustic Impedance Measurements of a Perforate Liner," *15th AIAA/CEAS Aeroacoustics Conference, AIAA Paper 2009*, Vol. 3301, 2009.

[10]Busse-Gerstengarbe, S., Bake, F., Enghardt, L., and Jones, M. G., "Comparative study of impedance eduction methods, Part 1: DLR tests and methodology," *19th AIAA/CEAS Aeroacoustics Conference*, 2013, pp. 2013–2124.

[11]Primus, J., Piot, E., Simon, F., Jones, M. G., and Watson, W. R., "ONERA-NASA cooperative effort on liner impedance eduction," *Proceedings of the 16th AIAA/CEAS Aeroacoustics Conference*, 2013.

[12]Buot de lEpine, Y., Chazot, J.-D., and Ville, J.-M., "Bayesian identification of acoustic impedance in treated ducts," *The Journal of the Acoustical Society of America*, Vol. 138, No. 1, 2015, pp. EL114–EL119.

[13]Scofano, A., Murray, P. B., and Ferrante, P., "Back-Calculation of Liner impedance using Duct Insertion Loss Measurements and FEM Predictions," *AIAA Paper*, Vol. 3534, 2007, pp. 2007.

[14]Bogey, C. and Bailly, C., "A family of low dispersive and low dissipative explicit schemes for flow and noise computations," *Journal of Computational Physics*, Vol. 194, No. 1, 2004, pp. 194–214.

[15]Berland, J., Bogey, C., Marsden, O., and Bailly, C., "High-order, low dispersive and low dissipative explicit schemes for multiple-scale and boundary problems," *Journal of Computational Physics*, Vol. 224, No. 2, 2007, pp. 637–662.

[16]Bogey, C., De Cacqueray, N., and Bailly, C., "A shock-capturing methodology based on adaptative spatial filtering for high-order non-linear computations," *Journal of Computational Physics*, Vol. 228, No. 5, 2009, pp. 1447–1465.

[17]Bogey, C. and Bailly, C., "Three-dimensional non-reflective boundary conditions for acoustic simulations: far field formulation and validation test cases," *Acta Acustica united with Acustica*, Vol. 88, No. 4, 2002, pp. 463–471.

[18]Rienstra, S. W., "Impedance models in time domain, including the extended Helmholtz resonator model," *AIAA Paper*, 2006, pp. 2006–2686.

[19]Dragna, D. and Blanc-Benon, P., "Physically admissible impedance models for time-domain computations of outdoor sound propagation," *Acta Acustica united with Acustica*, Vol. 100, No. 3, 2014, pp. 401–410.

[20]Li, X. Y., Li, X. D., and Tam, C. K. W., "Improved multipole broadband time-domain impedance boundary condition," *AIAA Journal*, Vol. 50, No. 4, 2012, pp. 980–984.

[21]Troian, R., Dragna, D., Bailly, C., and Galland, M.-A., "Broadband liner impedance eduction for multimodal acoustic propagation in the presence of a mean flow," *Journal of Sound and Vibrations*, 2016, under review.

[22]Deb, K., Pratap, A., Agarwal, S., and Meyarivan, T., "A fast and elitist multiobjective genetic algorithm: NSGA-II," *Evolutionary Computation, IEEE Transactions on*, Vol. 6, No. 2, 2002, pp. 182–197.